J Ind Microbiol Biotechnol
DOI 10.1007/s10295-016-1802-2

FERMENTATION, CELL CULTURE AND BIOENGINEERING

Functional characterization of a geraniol synthase-encoding gene from *Camptotheca acuminata* and its application in production of geraniol in *Escherichia coli*

Fei Chen[1,3] · Wei Li[1,3] · Liangzhen Jiang[1] · Xiang Pu[1,3] · Yun Yang[1,3] · Guolin Zhang[1] · Yinggang Luo[1,2]

Received: 22 April 2016 / Accepted: 20 June 2016

Abstract Geraniol synthase (GES) catalyzes the conversion of geranyl diphosphate (GPP) into geraniol, an acyclic monoterpene alcohol that has been widely used in many industries. Here we report the functional characterization of CaGES from *Camptotheca acuminata*, a camptothecin-producing plant, and its application in production of geraniol in *Escherichia coli*. The full-length cDNA of CaGES was obtained from overlap extension PCR amplification. The intact and N-terminus-truncated CaGESs were overexpressed in *E. coli* and purified to homogeneity. Recombinant CaGES showed the conversion activity from GPP to geraniol. To produce geraniol in *E. coli* using tCaGES, the biosynthetic precursor GPP should be supplied and transferred to the catalytic pocket of tCaGES. Thus, *ispA*(S80F), a mutant of farnesyl diphosphate (FPP) synthase, was prepared to produce GPP via the head-to-tail condensation of isoprenyl diphosphate (IPP) and dimethylallyl diphosphate (DMAPP). A slight increase of geraniol production was observed in the fermentation broth of the recombinant *E. coli* harboring t*CaGES* and *ispA*(S80F). To enhance the supply of IPP and DMAPP, the encoding genes involved in the whole mevalonic acid biosynthetic pathway were introduced to the *E. coli* harboring tCaGES and the *ispA*(S80F) and a significant increase of geraniol yield was observed. The geraniol production was enhanced to 5.85 ± 0.46 mg L^{-1} when another copy of *ispA*(S80F) was introduced to the above recombinant strain. The following optimization of medium composition, fermentation time, and addition of metal ions led to the geraniol production of 48.5 ± 0.9 mg L^{-1}. The present study will be helpful to uncover the biosynthetic enigma of camptothecin and tCaGES will be an alternative to selectively produce geraniol in *E. coli* with other metabolic engineering approaches.

Keywords Geraniol synthase · *Camptotheca acuminata* · Geraniol · Camptothecin · Metabolic engineering · Fermentation

Introduction

Geraniol (Fig. 1), an acyclic monoterpene alcohol, is a widely used and commercially important small molecule in the flavor and fragrance industries [3, 16, 43]. Geraniol shows antimicrobial, antioxidant, anti-inflammatory, and insecticidal activities [3]. Recently, geraniol was suggested to represent a new class of chemoprevention agents for cancer. Geraniol was also considered as a gasoline alternative superior to ethanol due to its low hygroscopicity, high energy content, and relatively low volatility [28, 43].

Geraniol is biosynthetically derived from geranyl diphosphate (GPP, Fig. 1), catalyzed by geraniol synthase (GES) featuring a common ionization-dependent reaction mechanism [2]. GPP is generated from the head-to-tail

Electronic supplementary material The online version of this article (doi:10.1007/s10295-016-1802-2) contains supplementary material, which is available to authorized users.

✉ Yinggang Luo
yinggluo@cib.ac.cn

[1] Center for Natural Products Research, Chengdu Institute of Biology, Chinese Academy of Sciences, Chengdu 610041, People's Republic of China

[2] State Key Laboratory of Bioorganic and Natural Products Chemistry, Shanghai Institute of Organic Chemistry, Chinese Academy of Sciences, Shanghai 200032, People's Republic of China

[3] University of Chinese Academy of Sciences, Beijing 100049, People's Republic of China

Published online: 27 June 2016

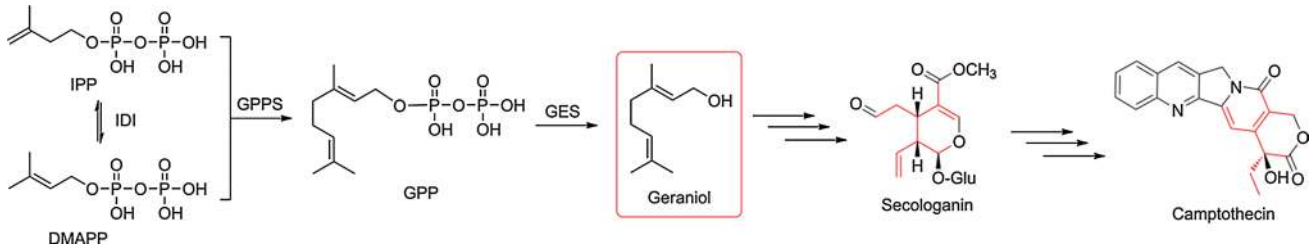

Fig. 1 The biosynthetic pathways of geraniol and its integration into secologanin and camptothecin in *Camptotheca acuminata*. The chemical structure of geraniol was highlighted in a *red rectangular frame* and the geraniol moieties incorporated into secologanin and camptothecin were highlighted in *red*. *IPP* isopentenyl diphosphate, *DMAPP* dimethylallyl diphosphate, *GPP* geranyl diphosphate, *IDI* IPP DMAPP isomerase, *GPPS* geranyl diphosphate synthase, *GES* geraniol synthase

condensation of the universal five-carbon precursors, isopentenyl diphosphate (IPP, Fig. 1) with its isomer dimethylallyl diphosphate (DMAPP, Fig. 1) [10, 20]. In turn, IPP and DMAPP are synthesized from the plastidial 2-*C*-methylerythritol 4-phosphate (MEP) pathway or the cytoplasmic mevalonic acid (MVA) pathway [7, 20].

The first cDNA encoding GES was cloned from the peltate glands of *Ocimum basilicum*, a geraniol-producing sweet basil and the resulting protein was functionally characterized to convert GPP into geraniol [12]. The GES-encoding genes had been cloned from several geraniol-producing plants [6, 13, 17, 21, 38, 41]. However, CrGES was cloned from *Catharanthus roseus*, the anticancer vincristine and vinblastine-producing plant [34]. It was demonstrated that the CrGES-catalyzed geraniol generation is a key step in the biosynthesis of monoterpenoid indole alkaloids (MIAs) such as the above mentioned vinca alkaloids and camptothecin [34, 37]. The iridoid glycoside secologanin from the geraniol moiety is condensed with tryptamine to afford strictosidine that is the common intermediate of all MIAs, including anticancer drugs camptothecin (Fig. 1), vincristine, and vinblastine [26, 36]. Herein we report the molecular cloning, heterologous overexpression, and functional characterization of a GES-encoding gene from *Camptotheca acuminata*, a camptothecin-producing plant in which geraniol is the biosynthetic precursor of secologanin and camptothecin (Fig. 1). The full-length cDNA of CaGES was obtained from two-round overlap extension PCR (OEPCR) amplification using the DNA fragments from conserved cloning, 5′- and 3′-rapid amplification of cDNA ends (RACE). The intact and N-terminus-truncated CaGES were overexpressed in *E. coli*, purified to homogeneity, and biochemically characterized. The CaGES exhibited the ability to convert GPP to geraniol. Different recombinant *E. coli* harboring tCaGES and *ispA*(S80F) (a mutant of FPP synthase that can produce GPP from IPP and DMAPP), with or without the encoding genes involved in the whole MVA biosynthetic pathway for IPP and DMAPP, were grown and fermented using two-phase fermentation method to produce geraniol. The geraniol was accumulated to 48.5 ± 0.9 mg L^{-1} under the present experimental conditions.

Materials and methods

Plant materials, seedling growth, and total RNA isolation

The *C. acuminata* seeds collection, seedling growth, and total RNA isolation were performed according to the reported procedures [30].

RT-PCR and nested PCR amplification of the core amplicon of CaGES

Two pairs of specific primers, CaGES-F1/R1 and CaGES-F2/R2 (Table 1), were designed for RT-PCR and following nested PCR amplification, respectively, on the basis of the nucleotide sequence of the annotated CaGES from the transcriptome data of *C. acuminata* (http://medicinalplantgenomics.msu.edu). The primers (Table 1) were synthesized, purified, and authenticated by Sangon Biotech (Shanghai) Co., Ltd. Using the template total RNA and CaGES-F1/R1 primers, the CaGES partial DNA was obtained from RT-PCR amplification with One Step RNA PCR Kit [Tiangen Biotech (Beijing) Co., Ltd., China], following the standard RT-PCR program: 1 cycle of 50°°C for 30 min, 1 cycle of 94 °C for 2 min, 35 cycles of 94 °C for 60 s, 48 °C for 30 s, and 65 °C for 2 min followed by a final extension at 65 °C for 10 min in a thermal cycler (Eppendorf AG, Hamburg, Germany). The amplified PCR products were gel-purified and used as a template DNA for the second-round PCR amplification with CaGES-F2/R2 primers, following the standard PCR program: 1 cycle of 94 °C for 3 min, 35 cycles of 94 °C for 30 s, 50 °C for 30 s, and 72 °C for 30 s followed by a final extension at 72 °C for 10 min. The amplified PCR products were gel-purified

Table 1 List of primers used in the study

Primer code	Sequence (5′–3′)	Direction	Application
CaGES-F1	GCATGTTGAGTTTATATGAAGC	Forward	Core amplicon amplification
CaGES-R1	AGTTCCCAAATCATCCCAG	Reverse	
CaGES-F2	TACTAGTTCTTGATGACATCTTTGAC	Forward	
CaGES-R2	CCCCATTTTCTATATATTCCTCT	Reverse	
3′-RACE-CaGES-GSP1	GGATGGAATGTGGTCCCATAC	Forward	3′-RACE
3′-RACE-CaGES-GSP2	CATGATTGAAGGCTTCCAAGCTGAGGC	Forward	
5′-RACE-CaGES-GSP1	CATGTCTATCCACGTCCTCTTTAGGTATGGGACC	Reverse	5′-RACE
5′-RACE-CaGES-GSP2	TGGGTAAAGCGGACAAGTTCATCTAATG	Reverse	
ORF-F	ATGGCTTGCATGAGTGTTTCTT	Forward	Full-length cloning
ORF-R	TTAGAGAATGGGAGTGAAGAACAATG	Reverse	
CaGES-BS-F	CGGGATCCGATGGCTTGCATGAG	Forward	Overexpression
CaGES-BS-R	ACGCGTCGACTTAGAGAATGGGAGTG	Reverse	
tCaGES-BS-F	CGGGATCCGGCTACTTCAACTGCAAC	Forward	
rtCaGES-F	TGATGGGGCAAGGAGTTACAGATG	Forward	Quantitative real-time PCR analysis
rtCaGES-R	CTCTCTCATAAACAGCTCAATGCTCG	Reverse	
S80F-F	GTGTATCCACGCTTACTTTTTAATTCATGATGATT	Forward	Site-mutagenesis
S80F-R	AATCATCATGAATTAAAAAGTAAGCGTGGATACAC	Reverse	
ispA-pBb-F	CCCAAGCTTGTGTCCTAGTTGTCAGCG	Forward	pBbA5c-MevT(CO)-MBIS (CO, *ispA*(S80F))
ispA-pBb-R	CGGGATCCTTATTTATTACGCTGGATG	Reverse	
ispA-pET-F	CGGGATCCGATGGACTTTCCGCAGCAAC	Forward	pETDuet-1-*ispA*(S80F)
ispA-pET-R	ACGCGTCGACTTATTTATTACGCTGGATG	Reverse	

and ligated into the pGM-T vector (Tiangen), according to the manufacturer's instruction. The *E. coli* DH5α competent cells were chemically transformed with the constructs and sequenced in Sangon Biotech (Shanghai) Co., Ltd. The nucleotide sequences were analyzed using the similarity BLAST search program.

Rapid amplification of cDNA ends (RACE) of CaGES

The gene-specific primers 3′-RACE-CaGES-GSP1 and -GSP2 (Table 1) were designed on the basis of the nucleotide sequence of the above confirmed amplicon of CaGES. The two primers were used with 3′-RACE outer and 3′-RACE inner primers supplied from Takara 3′-Full RACE Core Set [Takara Biotechnology (Dalian) Co., Ltd., China], respectively, to get the 3′-end of CaGES, according to the manual instructions. Briefly, the first strand cDNA mixture was synthesized using the template total RNA and 3′-RACE-Adaptor with PrimeScript™ RTase (Takara). Subsequent PCR amplification was performed using the first strand cDNA mixture as template and 3′-RACE-CaGES-GSP1 and 3′-RACE outer primers to obtain the 3′-end of CaGES, following the cycling conditions: 1 cycle of 94 °C for 3 min, 35 cycles of 94 °C for 30 s, 53 °C for 1 min, 72 °C for 40 s followed by a final extension at 72 °C for 10 min. The amplification products were gel-purified and used as template for nested PCR with 3′-RACE-CaGES-GSP2 and 3′-RACE inner primers, following the cycling conditions: 1 cycle of 94 °C for 3 min, 35 cycles of 94 °C for 30 s, 65 °C for 1 min, 72 °C for 40 s followed by a final extension at 72 °C for 10 min. The amplification products were gel-purified and ligated into the pGM-T vector. The *E. coli* DH5α competent cells were chemically transformed with the constructs following the procedure mentioned above. The nucleotide sequence of the 3′-end of CaGES was sequenced in Sangon Biotech Co., Ltd.

The 5′-end of CaGES was obtained using 5′-RACE methodology, according to the manual instructions of SMARTer™ RACE cDNA amplification kit from Clontech Laboratories, Inc (a member of Takara Bio Group). First, the total mRNA was purified from total RNA using the poly(A) mRNA purification kit (Sangon). The 5′-CDS Primer A was used as an adaptor and the purified mRNA as template to afford the 5′-RACE-Ready-cDNA with SMARTScribe Reverse Transcriptase. Touchup PCR amplification of the 5′-RACE-Ready-cDNA was performed using 5′-RACE-CaGES-GSP1 and universal Primer A mix as primers to afford the 5′-end of CaGES, following the cycling conditions: 1 cycle of 94 °C for 3 min, 5 cycles of 94 °C for 30 s, 55 °C for 1 min, 72 °C for 1 min 20 s; 5 cycles of 94 °C for 30 s, 58 °C for 1 min, 72 °C for 1 min 20 s; 5 cycles of 94 °C for 30 s, 61 °C for 1 min, 72 °C for 1 min 20 s; 20

cycles of 94 °C for 30 s, 70 °C for 1 min, 72 °C for 1 min 20 s followed by a final extension at 72 °C for 10 min. The PCR products were gel-purified, and used as template for the second-round touchdown PCR amplification using 5′-RACE-CaGES-GSP2, and NUP as primers, following the cycling conditions: 1 cycle of 94 °C for 3 min; 15 cycles of 94 °C for 30 s, 63 °C for 1 min, 72 °C for 1 min 10 s; 10 cycles of 94 °C for 30 s, 60 °C for 1 min, 72 °C for 1 min 10 s; 5 cycles of 94 °C for 30 s, 55 °C for 1 min, 72 °C for 1 min 10 s followed by a final extension at 72 °C for 10 min. The amplification products were gel-purified and ligated into the pGM-T vector. The *E. coli* DH5α competent cells were chemically transformed with the constructs and sequenced following the procedure mentioned above.

Full-length cDNA cloning of CaGES

The full-length cDNA of CaGES was obtained from two-round overlap extension PCR (OEPCR) amplification. Briefly, the 5′-end fragment and the conserved amplicon of CaGES were used as template, and ORF-F and CaGES-R2 as primers to afford fragment A of CaGES by OEPCR, following the cycling conditions: 1 cycle of 94 °C for 3 min; 35 cycles of 94 °C for 30 s, 52 °C for 1 min, 72 °C for 1 min 15 s followed by a final extension at 72 °C for 10 min. While using CaGES-F2 and ORF-R as primers, OEPCR of the conserved fragment and the 3′-end product of CaGES afforded fragment B of CaGES, following the cycling conditions: 1 cycle of 94 °C for 3 min; 35 cycles of 94 °C for 30 s, 52 °C for 1 min, 72 °C for 45 s followed by a final extension at 72 °C for 10 min. The full-length of CaGES was obtained from the second-round OEPCR using fragments A and B as template, ORF-F and ORF-R as primers, following the cycling conditions: 1 cycle of 94 °C for 3 min; 35 cycles of 94 °C for 30 s, 55 °C for 1 min, 72 °C for 1 min 40 s followed by a final extension at 72 °C for 10 min. The amplification products were gel-purified and ligated into the pGM-T vector. The *E. coli* DH5α competent cells were chemically transformed with the constructs and sequenced following the procedure mentioned above. The cDNA sequence of CaGES was deposited at GenBank under accession number KT633829.

Bioinformatic analyses and 3-dimensional structure prediction of CaGES

The bioinformatics analyses and 3-dimensional structure prediction of CaGES were performed according to the reported procedures [30].

Quantitative real-time PCR analysis of *CaGES*

To quantitate the relative expression level of CaGES in different plant tissues, the *C. acuminata* seedling growth, total RNA extraction, cDNA synthesis, real-time PCR amplification and analysis were performed, according to the reported procedures with minor modification [30]. For the experimental procedures in detail, see the Supplementary materials.

Heterologous overexpression and purification of CaGES

The primers CaGES-BS-F, tCaGES-BS-F, and CaGES-BS-R primers (Table 1) were designed and synthesized to amplify the intact (using CaGES-BS-F and -R as primers) and truncated (using tCaGES-BS-F and CaGES-BS-R as primers) CaGES from the full-length CaGES by PCR using a HiFi Taq DNA polymerase (TransGen Biotech (Beijing) Co., Ltd., China). The PCR conditions used were: 1 cycle of 94 °C for 3 min, 35 cycles of 94 °C for 30 s, 65 °C for 30 s, and 72 °C for 1 min 40 s followed by a final extension at 72 °C for 10 min. The PCR products were gel-purified, digested with *Bam*HI and *Sal*I endonucleases, and subcloned into pETDuet-1 vector digested with the same endonucleases to afford the expression constructs. The *E. coli* BL21(DE3) competent cells were chemically transformed with the expression constructs to afford the recombinant strains.

For protein overexpression, a single colony of recombinant strain was inoculated into 5 mL of Luria–Bertani (LB: tryptone, 10 g L^{-1}; NaCl, 10 g L^{-1}; and yeast extract, 5 g L^{-1}) broth containing 100 μg mL^{-1} of ampicillin and incubated overnight at 37 °C and 200 rpm in a shaking incubator. An aliquot culture (1 mL) was inoculated into 500 mL of LB broth supplemented with 100 μg mL^{-1} of ampicillin and incubated at 37 °C and 200 rpm. When the optical density (OD_{600nm}) of the culture reached 0.8, 1 mM of isopropyl β-D-1-thiogalactopyranoside (IPTG; Sangon) was added into the culture to induce the overexpression of the recombinant protein. The culture was incubated at 20 °C for another 17 h and 160 rpm. Cells were harvested by centrifugation at 4000 rpm for 15 min at 4 °C, washed twice with PBS buffer (50 mM Na_2HPO_4, 300 mM NaCl, 2 % glycerol, 10 mM β-mercaptoethanol, adjusted to pH 7.5 with NaOH, 4 °C), re-suspended in the same buffer containing 1 mg mL^{-1} lysozyme and 1 mM phenylmethylsulfonyl fluoride, and kept at 4 °C for 30 min. The suspended cells were sonicated on ice-bath followed by centrifugation at 10,000 rpm for 30 min at 4 °C. The supernatant was incubated with nickel-nitrilotriacetic acid resin (Sangon Biotech) for 30 min on ice-bath. The mixture of supernatant and resin was loaded on to a gravity-flow column and eluted with PBS buffer containing different concentrations of imidazole (10, 50, and 250 mM). The purified protein was desalted by dialysis membranes (Sangon) with PBS buffer (50 mM Na_2HPO_4, 150 mM NaCl, 20 % glycerol, pH 7.5, and 4 °C) and concentrated by

ultrafiltration using an Amicon Ultra 30 K MWCO centrifugal filter (Merck Millipoe Ltd., USA). The purified protein was stored with PBS buffer containing 20 % glycerol at −20 °C. The purified protein samples were analyzed on 10 % SDS-PAGE and their concentrations were estimated using the ε_{280nm} calculated from ExPASY ProtParam as follows: CaGES (ε_{280nm} = 93,780 M^{-1} cm^{-1}) and tCaGES (ε_{280nm} = 82,530 M^{-1} cm^{-1}).

Enzymatic activity assay and characterization of GES properties

The general enzymatic activity assays were performed in 50 μL PBS buffer (50 mM Na_2HPO_4, 150 mM NaCl, 10 % glycerol, pH 7.5) containing 1 mM $MgSO_4$, 0.1 mM $MnSO_4$, 50 μM GPP (purity ≥95 %, Sigma-Aldrich, USA), and 0.4 μM tCaGES. The reaction was initiated by the addition of GPP. The reaction mixture was incubated at 32 °C and an aliquot of the reaction mixture was quenched by adding 1 volume of chilled CH_3OH at 10, 30, 60, and 120 min, respectively.

Referring to the standard geraniol, the formation of geraniol from the enzymatic reaction was determined by HPLC equipped with an Altima C_{18} analytic column (250 × 4.6 mm, 5 μm). The mobile phase consisted of acetonitrile and H_2O and followed an isocratic elution (43:57), at a flow rate of 1 mL min^{-1} at 35 °C, monitored by a diode array detector.

The pH optimum for tCaGES activity was determined in different buffer systems with varying pH values. The reactions were performed in PBS buffer (50 mM Na_2HPO_4, 150 mM NaCl, 10 % glycerol, pH 6.0–7.5), 50 mM Tris–HCl with pH 8.0–8.5, and 50 mM Gly–NaOH buffer with pH 9.0–10.0. To investigate the effects of temperature on the catalytic activity of tCaGES, the purified enzyme was incubated at 0–45 °C for 30 min first and assayed its enzymatic activity using the general conditions mentioned above. Divalent metal ions Mg^{2+} and Mn^{2+} with different concentrations were added to the reaction mixture and assayed the enzymatic activity using the general conditions mentioned above.

To determine the kinetic parameters of tCaGES, the reaction was performed in 100 μL PBS buffer (50 mM Na_2HPO_4, 150 mM NaCl, 10 % glycerol, pH 7.5) containing 1 mM $MgSO_4$, 0.1 mM $MnSO_4$, 0.5 μM tCaGES, and GPP with different concentrations (0, 5, 10, 20, 30, 40, 80, and 120 μM). The kinetic constants were calculated with nonlinear regression analysis using Origin 9.0 software.

Quantitation and characterization of the product from the CaGES-catalyzed reaction

A standard geraniol curve was established to quantitate the formation of geraniol by HPLC. Briefly, standard geraniol solutions with 0, 10, 20, 40, 60, and 100 μM were prepared and subjected to HPLC–DAD analyses using the methods described above. The calibration curve was made from the stock solutions using a linear fit for the relationship of the specific concentration of geraniol versus the corresponding peak area integral at 200 nm. Limits of determination and quantification were determined as signal/noise = 3 and 10, respectively.

The CaGES-catalyzed reaction product was further characterized by GC–MS analysis. A QP2010 Plus GC–MS system (Shimadzu, Japan) equipped with a DB-5MS (30 m × 0.25 mm, 0.25 μm) capillary column with electron impact mode. Helium was used as the carrier gas at a flow rate of 1 mL min^{-1}. The separation conditions were: split mode 5:1, injection volume 1 μL, and injector temperature 250 °C. The initial oven temperature is 80 °C, retaining 2 min, then linear gradient to 100 °C at a rate of 5 °C min^{-1} followed by a linear gradient to 150 °C at a rate of 3 °C min^{-1}, with the final oven temperature 260 °C at a rate of 5 °C min^{-1}, retaining 2 min. The enzymatic geraniol was identified by comparing its retention time and mass fragmentation patterns with that of standard geraniol.

Fermentation optimization for geraniol production in *E. coli* using tCaGES

To produce geraniol in *E. coli* using tCaGES, a GPP synthase-encoding gene and the foreign encoding genes involved in the whole MVA biosynthetic pathway were introduced into *E. coli* since it did not produce and accumulate GPP. Different constructs were prepared from various vectors. The t*CaGES* was inserted into plasmid pETDuet-1 to afford construct I. The commercially available vector pBbA5c-MevT(CO)-MBIS (CO, *ispA*) (http://www.addgene.org/35151/) containing *ispA*, a farnesyl diphosphate synthase (FPPS)-encoding gene, and the encoding genes involved in the whole MVA biosynthetic pathway was proven to accumulate FPP in *E. coli*. It was reported that GPP will be accumulated in *E. coli* when the serine-80 of *ispA* was mutated to phenylanine via site-mutagenesis method to afford *ispA*(S80F), a GPPS [25, 29]. Thus *ispA*(S80F) was obtained by site-mutagenesis using template *ispA* and S80F-F and -R primers (Table 1), and inserted into *Bam*HI/*Sal*I sites of pETDuet-1 vector. The open reading frame of t*CaGES* was subcloned into *Bgl*II/*Xho*I sites of pETDuet-1 harboring *ispA*(S80F) to generate plasmid pETDuet-1-*ispA*(S80F)-t*CaGES* (II). The construct III, pBbA5c-MevT(CO)-MBIS [CO, *ispA*(S80F)], was prepared by site-mutagenesis mentioned above. The vectors I, II, I + III, and II + III were chemically transformed into *E. coli* BL21(DE3) competent cells, respectively, to generate the corresponding recombinant strain.

Two-phase fermentation method was introduced to ferment the recombinant strains prepared above. Briefly, a single colony of the recombinant strain was inoculated into 5 mL of LB broth containing 100 μg mL^{-1} of ampicillin, followed by incubating overnight at 37 °C in a shaking incubator. An aliquot (100 μL) culture was inoculated into 100 mL of LB medium supplemented with 100 μg mL^{-1} of ampicillin under the circumstances of 37 °C and 200 rpm, until OD_{600} reached 0.8. IPTG (1 mM) was added to induce protein overexpression at 20 °C and 160 rpm, followed by replenishing $MgSO_4$ and $MnSO_4$ for facilitating reactions 30 min later. After another 30 min, 20 mL of *n*-decane was overlaid over 100 mL of culture broth to capture geraniol. The fermentation for geraniol production was performed at 20 °C and 160 rpm for different time intervals with initial supplementation of different concentrations of $MgSO_4$ (0.1–2.0 mM) and $MnSO_4$ (0.1–2.0 mM). The *n*-decane layer was then collected and quantitated to 20 mL. The production of geraniol was determined by HPLC–DAD analysis as mentioned above. For the recombinant strains from I + III and II + III, 34 μg mL^{-1} of chloramphenicol was added to the seeds and fermentation media. All experiments were performed in triplicate.

Seven media, including LB, TB (tryptone, 12 g L^{-1}; glycerol, 4 mL L^{-1}; and yeast extract, 24 g L^{-1}), 2XYT (tryptone, 16 g L^{-1}; yeast extract, 10 g L^{-1}; NaCl, 5 g L^{-1}; and glucose, 10 g L^{-1}), M9 (glucose, 2 g L^{-1}; $CaCl_2$, 0.1 mM; $MgSO_4$, 2.0 mM; 1 X trace element solution; and 1 X M9 salts), 2XYTPG (tryptone, 16 g L^{-1}; yeast extract, 10 g L^{-1}; NaCl, 5 g L^{-1}; KH_2PO_4, 7 g L^{-1}; K_2HPO_4, 3 g L^{-1}; and glucose, 18 g L^{-1}), NBS (KH_2PO_4, 3.5 g L^{-1}; K_2HPO_4, 5 g L^{-1}; $(NH_4)_2HPO_4$, 3.5 g L^{-1}; $MgSO_4{\cdot}7H_2O$, 0.25 g L^{-1}; $CaCl_2{\cdot}2H_2O$, 15 mg L^{-1}; thiamine, 0.5 mg L^{-1}; 1 mL L^{-1} trace metal solution; and glucose, 30 g L^{-1}), and R/2 (KH_2PO_4, 6.75 g L^{-1}; $(NH_4)_2HPO_4$, 2 g L^{-1}; citric acid, 0.85 g L^{-1}; $MgSO_4{\cdot}7H_2O$, 0.8 g L^{-1}, and 5 mL L^{-1} trace metal solution; supplemented with glucose, 10 g L^{-1} and $(NH_4)_2SO_4$, 3 g L^{-1}) were prepared to ferment the recombinant *E. coli* harboring plasmids II and III.

Results

Molecular cloning of CaGES and its bioinformatics properties

The nucleotide sequence of a candidate CaGES, Caa_locus_24394, could be retrieved from the transcriptome database of *C. acuminata* (http://medicinalplantgenomics.msu.edu). The deduced amino acid residues of Caa_locus_24394 contain a highly conserved aspartate-rich motif DDXXD (highlighted in yellow, Fig. 2) and a less conserved NSE/DTE motif with the consensus sequence (L,V)(V,L,A)(N,D)D(L,I,V)X(S,T)XXXE (highlighted in pink, Fig. 2). The two motifs were found in most, if not all, plant GESs and were suggested to be involved in the binding and metal-dependent ionization of the diphosphate substrate [6, 34]. However, the N-terminal RRX_8W motif presented in many plant monoterpene synthases (highlighted in green, Fig. 2) could not be found in the candidate CaGES. Thus, a homology cloning strategy was employed to clone the conserved domain of CaGES based on the results of multiple sequence alignment (Fig. 2). A 305-bp conserved fragment of CaGES was obtained from RT-PCR and following nested PCR amplification. Subsequent 3′- and 5′-RACE afforded the 3′- and 5′-flanking regions with 465-bp and 1177-bp fragments, respectively. The full-length cDNA of CaGES was obtained from the two-round OEPCR amplification, and its nucleotide sequence was confirmed by molecular cloning and subsequent DNA sequencing.

The full nucleotide sequence of CaGES is 1906-bp and Caa_locus_24394 is a partial fragment of CaGES (Fig. 2). The cDNA of CaGES contains a 1785-bp open reading frame (ORF) encoding for a 594-amino acid residue protein (Fig. 2). The ORF was flanked by an 81-bp 5′-untranslated region (UTR) and a 40-bp 3′-UTR. The nucleotide sequence of the full-length cDNA of CaGES was deposited in NCBI GenBank under the accession number KT633829. The amino acid residue sequence alignment revealed that the conserved DDXXD and NSE/DTE binding domains of the diphosphate substrate are present in CaGES (Fig. 2). The N-terminal transit peptide containing RRX_8W motif was suggested to be involved in the plastidic localization of GES and the directional transit peptide will be cleaved after the protein is inserted into the organelle [12]. Although RRX_8W motif is absent in CaGES (Fig. 2), the CaGES was predicted to be a plastid target monoterpene synthases by TargetP software (http://www.cbs.dtu.dk/services/TargetP/), owing to the hydrophobic characteristic of its amino acid residues. Similarity search showed that CaGES shares 32.0–56.4 % amino acid residue identities with characterized plant GESs. The phylogenetic tree showed that CaGES is close to CrGES (Fig. S1a, Supplementary materials), indicating the CaGES's involvement in the biosynthetic pathway of camptothecin, a member of MIAs. Based on the crystal structure of the limonene synthase from *Mentha spicata* (MsLS, a metal ion-dependent monoterpene cyclase catalyzes the conversion of GPP into limonene via ionization, rearrangement, and cyclization reactions) [11], the 3-D structure of CaGES was constructed and refined by employing KoBaMIN web service (Fig. S1b, Supplementary materials). The metal ion Mn^{2+} (highlighted as green ball, Fig. S1b, Supplementary materials) was predicted to be embraced by the conserved DDXXD (highlighted in yellow ribbon, Fig. 3b) and NSE/DTE motifs (highlighted

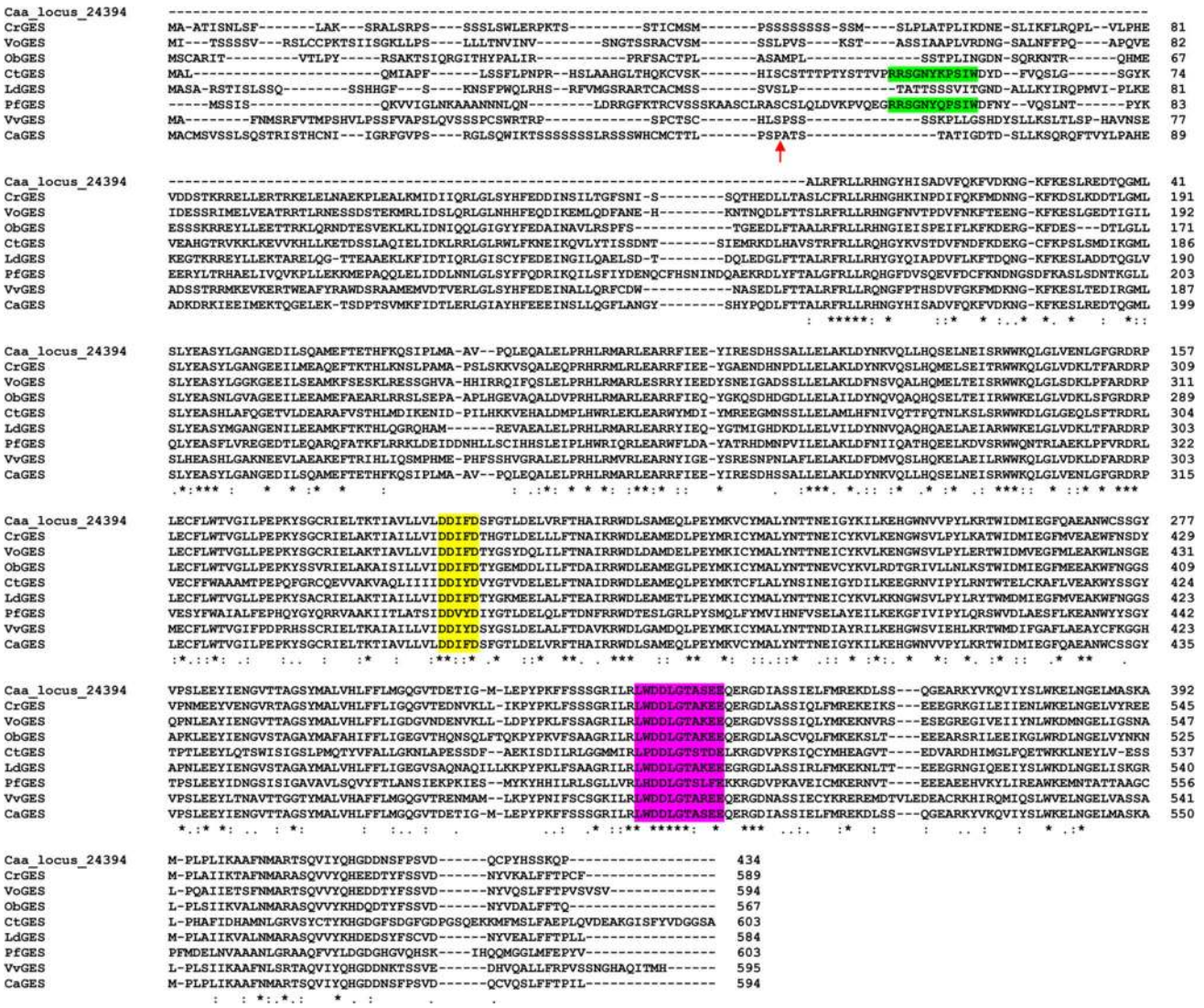

Fig. 2 Multiple sequence alignment of biochemically characterized plant GESs, predicted CaGES from *C. acuminata* transcriptome database, and CaGES presented in this study using Clustal Omega alignment tool. The highly conserved DDxxD region is highlighted in *yellow*. The less conserved NSE/DTE motif is highlighted in *pink*. The RRX_8W region is highlighted in *green*. The *red arrow* indicates the truncated position for tCaGES. Caa_locus_24394 was annotated as a CaGES and retrieved from the transcriptome database of *C. acuminata* (http://medicinalplantgenomics.msu.edu). CrGES from *Catharanthus roseus* (KF561459); VoGES from *Valeriana officinalis* (KF951406); ObGES from *Ocimum basilicum* (AY362553); CtGES from *Cinnamomum tenuipilum* (AJ457070); LdGES from *Lippia dulcis* (GU136162); PfGES from *Perilla frutescens* (DQ234300); VvGES from *Vitis vinifera* (NP_001267920)

in pink ribbon, Fig. S1b, Supplementary Materials) of CaGES. The real-time PCR amplification results showed that CaGES was expressed in all tissues of *C. acuminata* seedlings (Supplementary materials).

Heterologous overexpression and catalytic function of CaGES

Although the RRX_8W motif is absent in CaGES, analysis of the amino acid composition showed that hydrophobic, hydroxylated, and positively charged amino acid residues are rich in the N-terminus of CaGES, which is typical for a transit peptide [4]. The transit peptide has no influence on the catalytic activity of terpene synthases and it will be cleaved after their localization in plastid [2, 4]. Thus, the N-terminal 61 amino acid residues were truncated to generate tCaGES (the truncated position was indicated by a red arrow, Fig. 2). The intact and truncated *CaGES*s were subcloned into pETDuet-1 vector, and chemically transformed into *E. coli* BL21(DE3) to generate the recombinant strains. Overexpression and purification of CaGES and tCaGES using the identical procedure indicated that

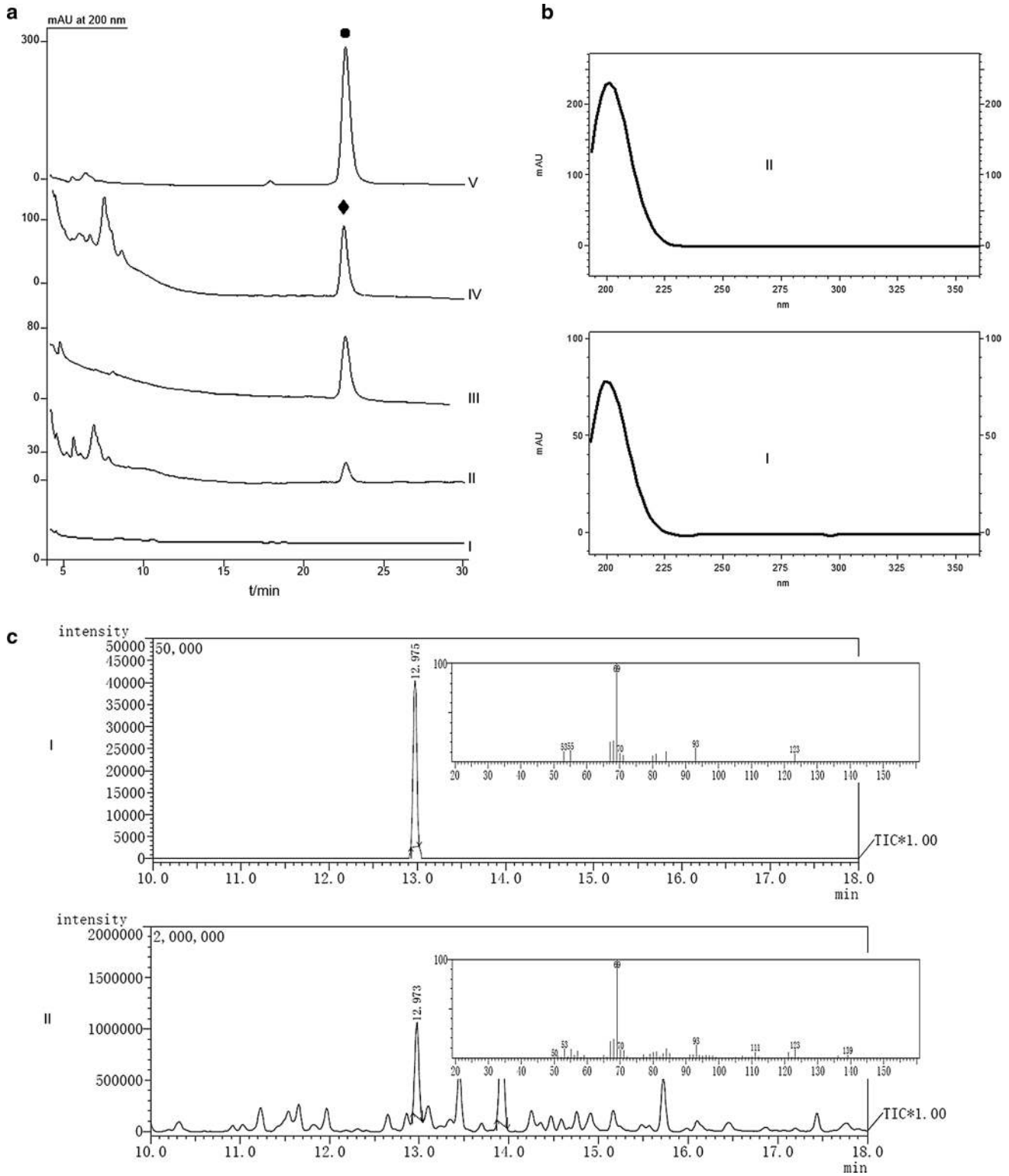

Fig. 3 Functional characterization of the recombinant CaGES. **a** HPLC–DAD analyses of the standard geraniol (*panel V*) and the enzymatic reaction mixture of tCaGES. The whole reaction containing $MgSO_4$, $MnSO_4$, and GPP was initiated by the addition of tCaGES. *Panel I*, the whole reaction with the boiled tCaGES; the enzymatic reaction was terminated at 5 min (*panel II*), 30 min (*panel III*), and 60 min (*panel IV*); *filled circle*, standard geraniol; *filled diamond*, product from the tCaGES-catalyzed reaction. **b** The UV spectra of the standard geraniol (*panel II*) and the enzymatic geraniol (*panel I*). **c** GC–MS analyses of the standard geraniol (*panel I*) and the enzymatic geraniol (*panel II*). The insets in *panels I* and *II* showed the fragmentation pattern of standard and enzymatic geraniol, respectively

tCaGES showed higher expression level than CaGES, and it will be easier to purify tCaGES to homogeneity (Fig. S2, Supplementary materials).

Geraniol can be separated and detected by HPLC–DAD analysis (panel V, Fig. 3a and panel II, Fig. 3b) using the isocratic acetonitrile and H_2O solvent system. Comparing with the authentic geraniol (panel V, Fig. 3a), enzymatic activity assays showed that no geraniol was detected when the general assay was performed with the boiled GES (panel I, Fig. 3a). Both CaGES and tCaGES showed time-dependent conversion of GPP to a new compound (panels II, III, and IV, Fig. 3a). This new product showed identical retention time (panels II, III, and IV, Fig. 3a) and UV profile (panel I, Fig. 3b) to those of the authentic geraniol (panel V, Fig. 3a and panel II, Fig. 3b). To further confirm the above results, GC–MS analysis was performed and the results showed that the new product has identical retention time and fragmentation ion pattern (panel II, Fig. 3c) with that of the authentic geraniol (panel I, Fig. 3c).

The pH values of the reaction buffer have significant effects on the catalytic activity of tCaGES (Fig. S3a, Supplementary materials). When the pH value of the buffer is 7.5, tCaGES shows the maximum catalytic activity (Fig. S3a, Supplementary materials). While tCaGES is stable at 5–25 °C for 30 min and it exhibits similar activity (Fig. S3b, Supplementary materials). However, tCaGES will lose 50 % activity after it was incubated at 45 °C for 30 min (Fig. S3b, Supplementary materials). No geraniol was detected when the metal ions Mg^{2+} and Mn^{2+} were absent in the standard enzymatic reactions (Fig. S3c, Supplementary materials), which suggested that tCaGES is a metal ion-dependent terpene synthase. The appropriate combination of Mg^{2+} and Mn^{2+} for tCaGES catalytic activity is 1 mM Mg^{2+} and 0.1 mM Mn^{2+} (Fig. S3c, Supplementary materials), which is in consistent with other characterized plant GESs [6, 12, 34]. The apparent kinetic parameters K_m and V_{max} of tCaGES for GPP were determined to be 89.5 ± 6.1 μM and 5.9 ± 0.2 μmol min^{-1} μM $protein^{-1}$, respectively (Fig. S3d, Supplementary materials).

Production of geraniol using tCaGES in *E. coli*

To produce geraniol in *E. coli*, different plasmids were constructed and chemically transformed into *E. coli* BL21(DE3) competent cells to generate the corresponding recombinant stains (Fig. 4a). Trace geraniol (0.022 ±

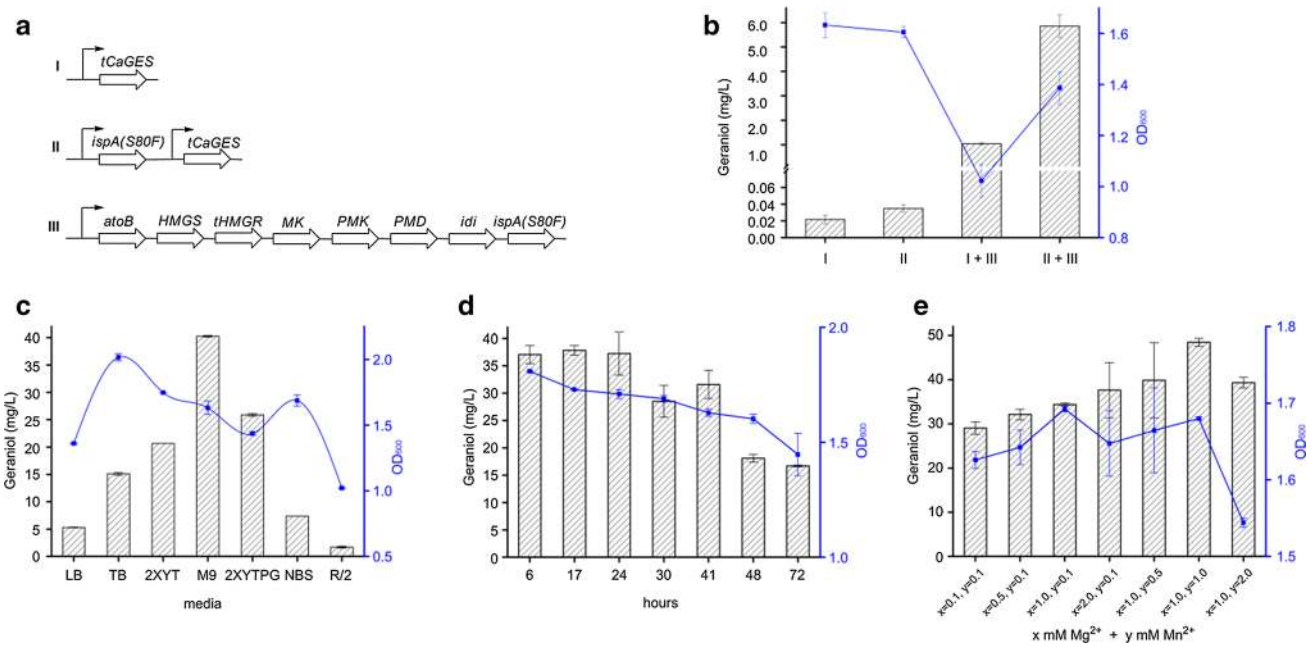

Fig. 4 Production of geraniol in *E. coli* using tCaGES. **a** The schematic representation of plasmids. I, pETDuet-1-t*CaGES*; II, pETDuet-1-*ispA*(S80F)-t*CaGES*; and III, pBbA5c-MevT(CO)-MBIS (CO, *ispA*(S80F)). **b** The geraniol yields (*column*) and the biomass (*blue line*) of the corresponding recombinant *E. coli* harboring different plasmids. The effects of fermentation media (**c**), time intervals (**d**), and the addition of metal ions with different concentrations (**e**) on the geraniol yield (*columns*) and the biomass (*blue lines*) of recombinant *E. coli*. The fermentation procedure can be found in the experimental section. In brief, 20 mL of *n*-decane was overlaid to the 100 mL of culture broth. When the planed fermentation was completed, the *n*-decane layer was collected, quantitated to 20 mL, and subjected to HPLC–DAD analysis. The total geraniol was calculated from the HPLC–DAD quantification of the *n*-decane layer. The geraniol yield was normalized to the 100–mL fermentation broth and stated in mg L^{-1} aqueous culture. The growth of *E. coli* was described in OD_{600}. It should be noted that in (**e**) the concentration of the metal ions below the graphs was added in addition to the 2.0–mM MgSO4 already present in the M9 medium

0.005 mg L^{-1}) was detected in the fermentation broth of the recombinant *E. coli* harboring only pETDuet-1-t*CaGES* (I, Fig. 4b), which was consistent with the previous report that *E. coli* cannot accumulate GPP [43]. To supply GPP for tCaGES to synthesize geraniol, the *ispA*(S80F) was inserted into the pETDuet-1 vector harboring t*CaGES* (II, Fig. 4a). A slight increase of geraniol yield (0.035 ± 0.004 mg L^{-1}) was obtained (II, Fig. 4b), which suggested that the supply of IPP and DMAPP is limited in *E. coli*. Thus, the encoding genes involved in the whole MVA biosynthetic pathway for the supply of IPP and DMAPP and *ispA*(S80F) (III, Fig. 4a) were introduced to the recombinant strain harboring pETDuet-1-t*CaGES*. The geraniol yield of the recombinant strain was significantly increased to 1.04 ± 0.04 mg L^{-1} (I + III, Fig. 4b), which confirmed that incorporation of the whole pathway for GPP biosynthesis will increase the geraniol production yield. A substantial increase of geraniol yield (5.85 ± 0.46 mg L^{-1}) was observed when another copy of *ispA*(S80F) was incorporated into the recombinant strain harboring pBbA5c-MevT(CO)-MBIS [CO, *ispA*(S80F)] and pETDuet-1-t*CaGES*, i.e., II + III (Fig. 4b).

Thus, the recombinant *E. coli* harboring plasmids II and III was set as the target strain for fermentation conditions optimization for geraniol production. M9 medium was found to be the best one in the present study (Fig. 4c). The high geraniol yield was obtained when the recombinant strain was fermented 17–24 h (Fig. 4d). The addition of 1 mM $MgSO_4$ and 1 mM $MnSO_4$ to the fermentation broth offered a higher geraniol yield (Fig. 4e). The geraniol production was increased to 48.5 ± 0.9 mg L^{-1} under the optimized fermentation conditions.

Discussion

Geraniol is a widely used acyclic simple alcohol in many fields. It is mainly produced in plants with its isomers such as linalool, oxidized derivatives like geranial and geranic acid, and glucose conjugates of these compounds. It is time consuming to purify geraniol from plant extracts. It will be very useful and cost-effective to selectively produce geraniol in simple organisms with high yield. Metabolic engineering has been proven to be a realistic alternative to improve yield and accessibility for natural products [15]. Transgenic tobacco with *VoGES* from *Valeriana officinalis* produced geraniol, hydroxygeraniol, and their glycoside forms [22, 31]. Although geraniol was the main product, the average of 13.7 μg g dryweight^{-1} and a maximum of 31.3 μg g dryweight^{-1} of geraniol were obtained [31]. Microbial organisms are versatile heterologous hosts for pharmaceutically important natural products via metabolic engineering biosynthetic pathways [24]. The geraniol production in recombinant yeast was increased to 36.04 mg L^{-1} [19]. Comparing with the heterologous hosts such as model plants and yeasts, *E. coli* is a favorable host for its easy growth, fermentation, and post-processing to produce geraniol [8, 9, 18, 22, 24, 31, 43]. However, *E. coli* itself cannot accumulate GPP and the supply of the isoprenoid precursors IPP and DMAPP is limited in *E. coli* [24]. The foreign genes for the biosynthesis of IPP, DMAPP, and GPP have to be introduced into *E. coli*. The present work showed that geraniol production was increased to 48.5 ± 0.9 mg L^{-1} by engineering tCaGES and the foreign genes mentioned above. The geraniol yield of this study is higher than those in transgenic tobacco and yeast; also, parallel to or higher than the yields of other terpenes production in metabolically engineered microorganisms [23, 32, 39, 40, 42]. Recently it has been demonstrated that deletion of YjgB, an endogenous dehydrogenase responsible for geraniol loss in *E. coli* MG1655, will increase geraniol production to 182.5 mg L^{-1} [38]. However, no geraniol analogues were detected in *E. coli* BL21(DE3) of this study, indicating that tCaGES is an alternative to selectively produce geraniol in *E. coli*. The difference may ascribe to the different type of *E. coli* host strains used for geraniol production. It should be noted that the yield of geraniol decreased after two days of fermentation (Fig. 4d). However, no geraniol analogues or derivatives were observed in the present experimental conditions, which may suggest that the geraniol was metabolized to other substances that cannot be detected in the present experimental conditions.

Carefully balancing the whole L-limonene biosynthetic pathway was evidenced the L-limonene production with a level of 430 mg L^{-1} in engineered *E. coli* [1]. In addition, the fed-batch fermentation was proved to increase the yields of other terpenes [23, 39, 40, 42]. Thus, this study will be an alternative to selectively produce geraniol in engineered *E. coli*, together with other metabolic engineering methods such as balancing the whole biosynthetic pathway and using fed-batch fermentation.

Clinically used camptothecin-type drugs are well known for their efficient anticancer effects against a broad band of tumor types such as small lung cancer and refractory ovarian cancer [5, 35]. Camptothecin, extracted and purified from plants *C. acuminata* in China and *Nothapodytes foetida* in India, is the starting material for chemical transformation to camptothecin-type drugs [19]. Thus the investigations of the biosynthetic mechanisms involved in the biosynthesis of camptothecin will be helpful to increase the production amount of camptothecin via plant molecular breeding, metabolic engineering, etc. [14, 27, 33]. The present work describes the molecular and biochemical facets for the generation of geraniol in *C. acuminata* that is a key biosynthetic step involved in camptothecin biosynthesis (Fig. 1). The results will facilitate to uncover the

biosynthetic enigma of camptothecin step by step, together with previous research efforts [30, 33].

Acknowledgments The authors wish to acknowledge the financial support in part by the Science and Technology Project for Outstanding Youths in Life Science (KSCX2-EW-Q-6) from the Chinese Academy of Sciences, the Applied and Basic Research Program of Sichuan Province (2015JY0058), and the 21172216 project from the National Natural Science Foundation of China. All authors have agreed to submit this manuscript to the Journal of Industrial Microbiology and Biotechnology.

References

1. Alonso-Gutierrez J, Chan R, Batth TS, Adams PD, Keasling JD, Petzold CJ, Lee TS (2013) Metabolic engineering of *Escherichia coli* for limonene and perillyl alcohol production. Metab Eng 19:33–41
2. Bohlmann J, Meyer-Gauen G, Croteau R (1998) Plant terpenoid synthase: molecular biology and phylogenetic analysis. Proc Natl Acad Sci USA 95:4126–4133
3. Chen W, Viljoen AM (2010) Geraniol—a review of a commercially important fragrance material. S Afr J Bot 76:643–651
4. Croteau R (1987) Biosynthesis and catabolism of monoterpenoids. Chem Rev 87:929–954
5. Demain AL, Vaishnav P (2011) Natural products for cancer chemotherapy. Microbiol Biotechnol 4:687–699
6. Dong L, Miettinen K, Goedbloed M, Verstappen FWA, Voster A, Jongsma MA, Memelink J, van der Krol S, Bouwmeester HJ (2013) Characterization of two geraniol synthase from *Valeriana officinalis* and *Lippia dulcis*: similar activity but difference in subcellular localization. Metab Eng 20:198–211
7. Eisenreich W, Rohdich F, Bacher A (2001) Deoxyxylulose phosphate pathway to terpenoids. Trends Plant Sci 6:78–84
8. Fischer MJC, Meyer S, Claudel P, Bergdoll M, Karst F (2011) Metabolic engineering of monoterpene synthesis in yeast. Biotechnol Bioeng 108:1883–1892
9. Fischer MJC, Meyer S, Claudel P, Perrin M, Ginglinger JF, Gertz C, Masson JE, Werck-Reinhardt D, Hugueney P, Karst F (2013) Specificity of *Ocimum basilicum* geraniol synthase modified by its expression in different heterologous system. J Biotechnol 163:24–29
10. Gao Y, Honzatko RB, Peters RJ (2012) Terpenoid synthase structure: a so far incomplete view of complex catalysis. Nat Prod Rep 29:1153–1175
11. Hyatt DC, Youn B, Zhao Y, Santhamma B, Coates RM, Croteau RB, Kang CH (2007) Structure of limonene synthase, a simple model for terpenoid cyclase catalysis. Proc Natl Acad Sci USA 104:5360–5365
12. Iijima Y, Gang DR, Fridman E, Lewinsohn E, Pichersky E (2004) Characterization of geraniol synthase from the peltate glands of sweet basil. Plant Physiol 134:370–379
13. Ito M, Honda G (2007) Geraniol synthase from perilla and their taxonomical significance. Phytochemistry 68:446–453
14. Kutchan TM (1995) Alkaloid biosynthesis—the basis for metabolic engineering of medicinal plants. Plant Cell 7:1059–1070
15. Lange BM, Ahkami A (2013) Metabolic engineering of plant monoterpenes, sesquiterpenes and diterpenes—current status and future opportunities. Plant Biotechnol J 11:169–196
16. Lapczynski A, Bhatia SP, Foxenberg RJ, Letizia CS, Api AM (2008) Fragrance material review on geraniol. Food Chem Toxicol 46:S160–S170
17. Liu J, Huang F, Wang X, Zhang M, Zheng R, Wang J, Yu D (2014) Genome-wide analysis of terpene synthase in soybean: functional characterization of GmTPS3. Gene 544:83–92
18. Liu J, Zhang W, Du G, Chen J, Zhou J (2013) Overproduction of geraniol by enhanced precursor supply in *Saccharomyces cerevisiae*. J Biotechnol 168:446–451
19. Lorence A, Nessler CL (2004) Camptothecin, over four decades of surprising findings. Phytochemistry 65:2735–2749
20. Mahmoud SS, Croteau R (2002) Strategies for transgenic manipulation of monoterpene biosynthesis in plants. Trends Plant Sci 7:366–373
21. Martin DM, Aubourg S, Schouwey MB, Daviet L, Schalk M, Toub O, Lund ST, Bohlmann J (2010) Functional annotation, genome organization and phylogeny of the grapevine (*Vitis vinifera*) terpene synthase gene family based on genome assembly, FLcDNA cloning, and enzyme assays. BMC Plant Biol 10:226
22. Masakapalli SK, Ritala A, Dong L, van der Krol AR, Oksman-Caldentey K, Ratcliffe RG, Sweetlove LJ (2014) Metabolic flux phenotype of tobacco hairy roots engineered for increase geraniol production. Phytochemistry 99:73–85
23. Mi J, Becher D, Lubuta P, Dany S, Tusch K, Schewe H, Buchhaupt M, Schrader J (2014) De novo production of the monoterpenoid geranic acid by metabolically engineered *Pseudomonas putida*. Microb Cell Fact 13:170
24. Morrone D, Lowry L, Determan MK, Hershey DM, Xu M, Peters RJ (2010) Increasing diterpene yield with a modular metabolic engineering system in *E. coli*: comparison of MEV and MEP isoprenoid precursor pathway engineering. Appl Microbiol Biotechnol 85:1893–1906
25. Ohnuma SI, Narita K, Nakazawa T, Ishida C, Takeuchi Y, Ohto C, Nishino T (1996) A role of the amino acid residue located on the fifth position before the first aspartate-rich motif of farnesyl diphosphate synthase on determination of the final product. J Biol Chem 271:30748–30754
26. Panjikar S, Stoeckigt J, O'Connor S, Warzecha H (2012) The impact of structural biology on alkaloid biosynthesis research. Nat Prod Rep 29:1176–1200
27. Peng ZH, Hu JJ, Li HS (2010) Application of biotechnology in research of camptothecin. Prog Modern Biomed 10:3175–3177
28. Peralta-Yahya PP, Keasling JD (2010) Advanced biofuel production in microbes. Biotechnol J 5:147–162
29. Peralta-Yahya PP, Ouellet M, Chan R, Mukhopadhyay A, Keasling JD, Lee TS (2011) Identification and microbial production of a terpene-based advanced biofuel. Nat Commun 2:483. doi:10.1038/ncomms1494
30. Qu X, Pu X, Chen F, Yang Y, Yang L, Zhang G, Luo Y (2015) Molecular cloning, heterologous expression, and functional characterization of an NADPH-cytochrome P450 reductase gene from *Camptotheca acuminata*, a camptothecin-producing plant. PLoS One 10:e0135397
31. Ritala A, Dong L, Imseng N, Seppänen-Laakso T, Vasilev N, van der Krol S, Rischer H, Maaheimo H, Virkki A, Brändli J, Schillberg S, Eibl R, Bouwmeester H, Oksman-Caldentey K (2014) Evaluation of tobacco (*Nicotiana tabacum* L. cv. Petit Havana SR1) hairy roots for the production of geraniol, the first committed step in terpenoid indole alkaloid pathway. J Biotechnol 176:20–28
32. Sarria S, Wong B, Martín HG, Keasling JD, Peralta-Yahya P (2014) Microbial synthesis of pinene. ACS Synth Bio 3:466–475
33. Shen SH, Liu JY, Hu JQ, Li XH, Wang LL (2011) Advances in studies on biosynthetic pathways of camptothecin and their synthases. Chin Trad Herbal Drugs 42:1862–1868
34. Simkin AJ, Miettinen K, Claudel P, Burlat V, Guirimand G, Courdavault V, Papon N, Meyer S, Godet S, St-Pierre B, Giglioli-Guicarc'h N, Fischer MJC, Memelink J, Clastre M (2013) Characterization of the plastidial geraniol synthase from Madagascar periwinkle which initiates the monoterpenoid branch of the alkaloid pathway in internal phloem associated parenchyma. Phytochemistry 85:36–43

35. Sirikantaramas S, Asano T, Sudo H, Yamazaki M, Saito K (2007) Camptothecin: therapeutic potential and biotechnology. Curr Pharm Biotechnol 8:196–202
36. Stöckigt J, Barleben L, Panjikar S, Loris EA (2008) 3D-Structure and function of strictosidine synthase—the key enzyme of monoterpenoid indole alkaloid biosynthesis. Plant Physiol Biochem 46:340–355
37. Sung PH, Huang FC, Do YY, Huang PL (2011) Functional expression of geraniol 10-hydroxylase reveals its dual function in the biosynthesis of terpenoid and phenylpropanoid. J Agric Food Chem 59:4637–4643
38. Vezzaro A, Krause ST, Nonis A, Ramina A, Degenhardt J, Ruperti B (2012) Isolation and characterization of terpene synthases potentially involved in flavor development of ripening olive (*Olea europaea*) fruits. J Plant Physiol 169:908–914
39. Willrodt C, David C, Cornelissen S, Bühler B, Julsing MK, Schmid A (2014) Engineering the productivity of recombinant *Escherichia coli* for limonene formation from glycerol in minimal media. Biotech J 9:1000–1012
40. Yang J, Nie Q, Ren M, Feng H, Jiang X, Zheng Y, Liu M, Zhang H, Xian M (2013) Metabolic engineering of *Escherichia coli* for the biosynthesis of alpha-pinene. Biotechnol Biofuels 6:60
41. Yang T, Li J, Wang H, Zeng Y (2005) A geraniol-synthase gene from *Cinnamomum tenuipilum*. Phytochemistry 66:285–293
42. Zhang H, Liu Q, Cao Y, Feng X, Zheng Y, Zou H, Liu H, Yang J, Xian M (2014) Microbial production of sabinene—a new terpene-based precursor of advanced biofuel. Microb Cell Fact 13:20
43. Zhou J, Wang C, Yoon S, Choi E, Kim S (2014) Engineering *Escherichia coli* for selective geraniol production with minimized endogenous dehyrogenation. J Biotechnol 169:42–50